# Quantum-Driven Artificial algae algorithm: A Novel Approach to MRI Brain segmentation

[1*]K S. Balamurugan, [2]M.Chandrasekhar, [3]R.Rajalakshmi, [4]H.Enthamizhselvi, [5]G. Kalyani, [6]Surendran R

[1*]Professor & Head, Department of Electronics and Communication Engineering, Koneru Lakshmaiah Karpaga vinayaga college of Engineering and Technology, Chengalpattu, Tamilnadu, India. profksbala@gmail.com

[2]Professor, Department of Mechanical Engineering, Chalapathi Institute of Engineering and Technology, Guntur, Andhra Pradesh, India. principal@chalapathiengg.ac.in

[3]Assistant Professor,Departmentof ECE, Pandian Saraswathi Yadav Engineering College, Sivaganga, Tamil Nadu, India. kbraji1985@gmail.com

[4]Assistant professor, Department of CSE, Karpaga vinayaga Engineering College, Chengalpattu, Tamilnadu, India. senthamizhselvikavi2830@gmail.com

[5]Research Associate, RuralCare Innovators LLP, Madurai, Tamil Nadu, India. ruralcareinnovators@gmail.com

[6]Department of CSE, Saveetha School of Engineering, Saveetha Institute of Medical and Technical Sciences, Chennai, 602105, India. surendran.phd.it@gmail.com

[1*]Corresponding Author profksbala@gmail.com

**Abstract**

A crucial step in medical image processing is MRI brain (BT) segmentation which requires finding and characterizing tumors in brain MRI data. This procedure is necessary for brain diagnosis, therapy planning and progression detection. Significant challenges include the possibility of imaging deviations and activity, in addition to variation in tumor forms, sizes and positions. We propose the Quantum Artificial Algae Algorithm (QAAA) for MRI BT segmentation in this research. Initially, we collected a dataset from Kaggle. The 253 MRI images in the Kaggle dataset include 155 s and 98 non- images and pixel value normalization is used as a preprocessing technique on the data to minimize intensity differences resulting from different treatments and to provide image comparability. The next step is to extract relevant features from the pre-processed data using the Gabor filter approach. It is a useful tool for evaluating MRI data in the context of identifying brain s. The suggested model uses a quantum-inspired approach to computation that addresses the differences between analysis and processing. Using quantum rotational gates, a group of people can first be rotated to a place where the ideal number could be

easily obtained. To assess that the suggested method works, we simulate using the Python 3.11 program. 98.3% accuracy, 98.2% precision, 98.6% specificity, 97.6% recall and 98% F1-score. We present interesting outcomes for MRI brain segmentation using our proposed QAAA approach.

**Keywords**

MRI brain (BT) segmentation**,** medical images, quantum computing,Quantum-Driven Artificial Algae Algorithm (QAAA).

**Introduction**

In the field of neurological imaging, MRI is an effective invisible technology that is useful for early disease detection, diagnosis and treatment planning (Senan et al. (2022)). MRI is an essential instrument in neurologists for diagnosing and segmenting brain s. Brain s are a serious health risk and indicate that accurate identification is essential for successful treatment (Kollam et al., 2023).

The method of differentiating various areas in the brain images that correspond to tumor tissues is known as MRI BT segmentation (Chahal et al. (2020)). Determining the size, location and features of the tumor is crucial for establishing a course of treatment and keeping updated on the disease's evolution (Chen et al.(2021) and Ali et al.(2022)). It can be achieved through the segmentation process. Conventional manual segmentation techniques require a lot of work and they are subjective, which results in variability across observers (Petralia et al. (2020)). Therefore, to improve the effectiveness and dependability of diagnosis, there is an increasing demand for automated and precise segmentation procedures (Kollem et. al (2023)).

Different MRI sequences, such as “T1-weighted and T2-weighted scans”, are used in the early phases of diagnosis to find anomalies in brain cells (Kurmi et al. (2020)). Furthermore, ingesting a substance that provides contrast, typically gallium, can produce contrast-enhanced images by making certain characteristics, such as blood arteries and tumor tissue, more visible (Tataei Sarshar et al.(2021) and Amran et al.(2022)).

Treatment planning greatly benefits from MRI's capacity to locate brain tumors (Magadza et al. (2021)). The precise location and size of the tumor can help medical practitioners to create more focused treatment plans, such as chemotherapy, intravenous radiation, or surgery (Wu et al. (2022)). In particular, deep learning and machine learning algorithms have changed the field of medical image analysis with the introduction of sophisticated computational techniques

(Yamanakkanavar et al. (2020)). By automating the segmentation process, these methods can reduce the need for human intervention while increasing the overall accuracy of tumor segmentation (Biratu et al. (2021)). These innovative methods are used by experts and medical professionals to create strong dependable models that can manage the complexity as well as unpredictability of brain tumor images (Haq et al. (2022)).

Despite there have been encouraging developments in MRI BT segmentation, there are certain restrictions. Among the challenges is the variety of tumor features, including size, form and location, which can prevent the creation of segmentation algorithms that are relevant to the instances. Another significant difficulty is the vulnerability of segmentation models to noise, imaging artifacts and variations in imaging methods. The generalization ability of models can be impacted by the limitations of varied and well-annotated datasets for training and validation.

To overcome these obstacles, further study is required to improve algorithms, strengthen robustness and promote cooperation to create uniform datasets that will increase the accuracy and usefulness of MRI BT segmentation in healthcare environments. The purpose of this work was to propose a new method for MRI brain tumor segmentation classified as the Quantum Artificial Algae Algorithm (QAAA).

***Key contributions***

These are the primary findings to be extracted from this MRI brain tumor segmentation study.

- To assess the Kaggle dataset, out of the 253 total MRI scans, 155 are aberrant tumor images and 98 are normal images.
- To ensure standardized and reliable information, preprocessing techniques such as pixel value normalization are employed.
- The Gabor filter method of feature extraction can be used to identify significant parameters for MRI BT segmentation.
- In addition, a novel method for MRI BT segmentation called QAAA is used. We evaluate the accuracy, precision, recall, specificity and f1-score of the experimental data.

This essay is divided into five pieces. In section 2, the pertinent works and their relationship to the study are covered. Section 3 provides the study methodologies, including the tactics and strategies that were employed. The research and their findings are presented in detail in section 4, with a focus on the key conclusions and discoveries. The study's main conclusions and ramifications are outlined in section 5, which serves as the conclusion.

**Related works**

A functionally segregated network that utilized an "encoder-decoder structure" was presented by Myronenko (2019)) to segment tumor portions from 3D MRIs. A variation of auto-encoder branches had been introduced to replicate the image as input, it generates to normalize the collective decoding and implement more restrictions to its stages based on an insufficient training collection.

Zhang et al.(2020) investigated the efficacy of the attention gate consideration module, which were developed, for the BT segmentation problem, a unique "Attention Gate Residual U-Net model known as AGResU-Net" was further provided. The findings of the experiments demonstrated that systems with awareness gateway units were, "Attention Gate U-Net (AGU-Net) along with AGResU-Net executed better than the U-Net and ResU-Net starting points", correspondingly.

Ottom et al. (2022) introduced a unique framework for segmenting '2D brain tumors in MRI images". It was based on "deep neural networks (DNN)" and data augmentation approaches. Znet, the suggested method, used encoder-decoder constructions, skip connections and data enhancement to spread the inherent connections of a relatively small amount of defined tumors such as dozens of "low-grade glioma (LGG)" patients to thousands of synthetic cases. Their test results indicated that the mean dice similarity coefficient was high.

Thaha et al. (2019) demonstrated the segmentation of MRI images using algorithms for optimization. Compact kernels assisted in the implementation of a complex structure. Assigning smaller weights to the entire system had a favorable impact on reducing excessive fitting. The experiment's outcome demonstrated superior performance when compared to existing approaches.

Srinivasa Reddy and Chenna Reddy (2021) proposed automated methods for the detection and categorization of brain tumors. The preprocessing phase categorization, extraction of features, selecting features and categorization were the five steps that make up the suggested task. Various metrics were used to analyze the results of the experiments. Experiments and results demonstrated how well the suggested strategy segments categorized brain tumors in magnetic resonance images.

Brahim et al. (2019) suggested evaluating several neural network topologies that exhibit potential in-depth to address these concerns. Their research led us to three ways, based on "2D

U-Net, 3D U-Net and cascaded neural networks", respectively. These techniques were contrasted by an additional unstructured method based on k-mean clustering. During the right set of strategies was applied, they were able to improve the Dice score outcomes of the baseline procedures.

Ballestar and Vilaplana (2020) presented voxel-wise uncertainty information using "data-augmentation (TTA) and test-time dropout (TTD)", respectively, which could be epistemological or algebraic. In addition, a hybrid strategy was put forth that aids in improving the segmentation accuracy. For objectives 1 and 3 about the segmentation of tumors and confidence estimate in the BraTS'20 challenge, the study's recommended modeling and variability assessment methods were used.

Kao et al. (2020) presented a novel approach for BT segmentation that combines location data with the most advanced patch-based neural networks available. They connected the previously developed brain parcellation atlas to the individual subject data in the "Montreal Neurological Institute (MNI)" space. Furthermore, their suggested ensemble outperforms "state-of-the-art networks in BraTS 2018" and outperformed them in classification achievement when contrasted with BraTS 2017 state-of-the-art systems.

Sheng et al. (2021) investigated the efficacy of higher-order statistical characteristics in BT segmentation applications and proposed a novel "second-order residual BT segmentation network", "SoResU-Net". Numerous experiments conducted on the "BraTS 2018 and BraTS 2019" datasets demonstrated that "SoResUNet" outperformed its beginning, particularly on core tumor and improving tumor categorization, highlighting the utility of "second-order statistical" characteristics in the brain segmentation of tumor applications.

Amian and Soltaninejad (2020) proposed a computerized "three-dimensional (3D) deep classification method for 3D pre-operative" MRI scan tumor detection. Two perpendicular simplifies with two separate solutions were included in the deep structure that was suggested for the task of segmentation. The findings demonstrated that the suggested approaches offer survival forecasting and offering categories.

Giacomello et al. (2020) presented "SegAN-CAT, an end-to-end Adversarial Network-based method for BT segmentation in Magnetic Resonance Images (MRI)". They proposed to enhance the efficiency of single-modality examples by implementing transferable learning across various comparison methods. Their findings were encouraging as they demonstrate that transferable

knowledge preserve produces superior results whenever one technique can be utilized, in addition to the fact that "SegAN-CAT can outperform SegAN" when all four techniques were accessible.

Colman et al. (2021) proposed a "2D deep residual Unet for brain MRI lesion segmentation with 104 convolutional layers (DR-Unet104)". In addition to a component of the "Multimodal BT segmentation (BraTS)" 2020 challenge, they assessed the recommended design and contrasted their approach with "DeepLabV3+ using a ResNet-V2–152" foundation.

Chen et al. (2020) presented a novel symmetry-combining "deep convolutional neural network" that can categorize brain tumors. By incorporating symmetric masks into multiple layers, their neural networks dubbed "Deep Convolutional Symmetric Neural Networks", or "DCSNNs expand classification connections founded on DCNNs. The dice similarity coefficient metric (DSC)" was used to assess the outcomes.

Khalil et al. (2020) proposed an accurate two-step "dragonfly algorithm (DA)" clustering method for extracting initial contouring points. The suggested approach for BT segmentation can be compared to "state-of-the-art techniques", as demonstrated by the outcomes of using it on 3D-MRI images from the multimodal BT segmentation challenge (BRATS) 2017" information set.

**Methodology**

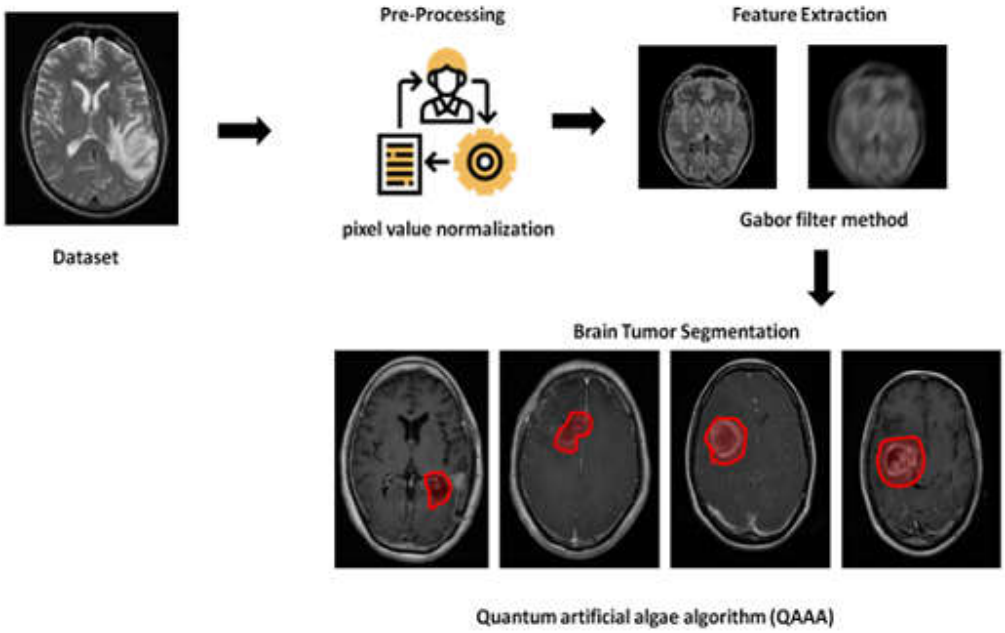


**Fig.1** The process of MRI brain tumor segmentation

(Source: Author)

Fig 1 illustrates the sequential progression of the steps, enhancing knowledge of the process. Developing a distinctive prototype for an MRI brain tumor will address a challenge in the field of research. We gathered Kaggle MRI image datasets. Data preprocessing involved pixel value normalization, feature extraction was performed using the Gabor filter approach and MRI BT segmentation was achieved using the proposed method.

***Dataset***

A publicly available MRI dataset is used to verify the proposed methodology. Kaggle was the source of the brain tumor dataset. There are 155 tumors (abnormal) and 98 non-tumor (normal) MRI images out of the 253 total in the Kaggle dataset. Training and testing are conducted on two sets of the brain tumor dataset. The training set makes up 70% of the dataset and the testing set comprises 30% (Kuraparthi et al. (2021)).

***Data preprocessing using pixel value normalization***

Pixel value normalization is essential in MRI brain tumor image processing to maintain consistency in intensity between scans. The dimensions of pixels are scaled to an acceptable range $(0\ to\ 1)$ using techniques including z-score normalization and min-max scaling. This reduces intensity differences from various treatments and ensures image comparability. Through meaningful pattern extraction it is made easier by normalization, tumor detection algorithms become more robust and accurate.

In computer vision applications, particularly in image processing and deep learning, pixel value normalization is a typical preprocessing step. The objective is to normalize an image's pixel values into a standard range, which will improve the model's learning process and enhance the training process' convergence and performance. Pixel value normalization can be achieved in several ways, but two common methods are as follows:

- **Min-Max Scaling:**

$$X_{normalized}=\frac{X-X_{min}}{X_{max-X_{min}}} \quad (1)$$

Where $X$ is the original pixel value, $X_{min}$ is the minimum pixel value in the image and $X_{max}$ is the maximum pixel value in the image.

The values of the normalized pixels will range between 0 and 1.

- **Z-score Standardization:**

$$X_{normalized}=\frac{X-\mu}{\sigma} \quad (2)$$

In the image, $\sigma$ represents the standard deviation of pixels, $\mu$ is the average of the pixel amounts and $X$ is the initial pixel quantity. The standardized pixels will have a standard deviation of 1 and a mean of 0. The process of normalization is a crucial step in machine learning model training as it guarantees that all input characteristics, such as pixel values, are on the same scale and prevents any specific feature from becoming dominant. It could strengthen the connection for training.

***Feature Extraction using the Gabor filter method***

Spatial frequency and orientation patterns are captured by filters in the Gabor filter-based feature extraction method used for MRI brain tumor identification. The filters attract attention to differences in texture linked to the presence of tumors. MRI images are convolved with Gabor filter kernels at various scales and orientations to provide a set of features. Machine learning algorithms use these features as input because they indicate local texture patterns. Because of its exceptional ability to identify minute features, the Gabor filter method is a useful tool for evaluating MRI data in the context of identifying brain tumors. Fig 2 shows the Gabor filter image.

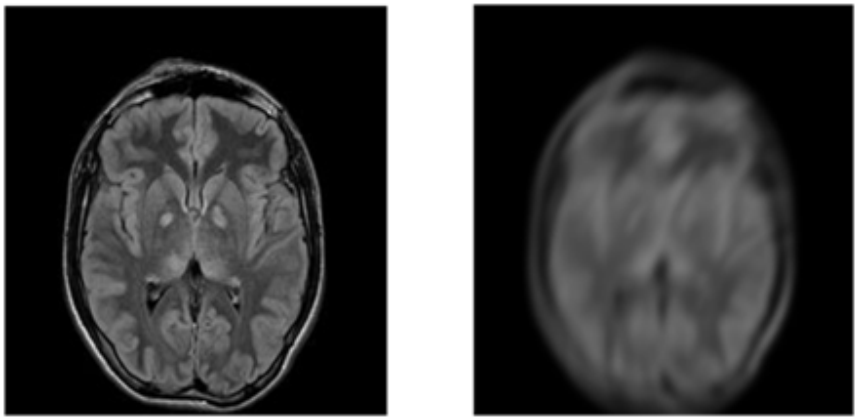

**Fig. 2** Gabor filtered image

(Source: https://www.kaggle.com/datasets/sartajbhuvaji/brain-tumor-classification-mri)

The consequence of the Fourier basis element and the Gaussian filter is a Gabor filter kernel. The Fourier basis makes the filter sensitive to particular spatial frequency and orientation elements of the image. For the filter to be spatially localized, a Gaussian filter is required. The convolution with the Gabor filter is comparable to the windowed Fourier transform in this regard. The Gabor filter, G(y, z), is demonstrated by the following equations.

$$G(x, y;\ \lambda, \theta, \psi, \sigma, \gamma) = exp\ -\ \frac{x'^2+\gamma^2 y'^2}{2\sigma^2} cos\left(2\pi \frac{x'}{\lambda} +\ \psi\right) \quad (3)$$

$$y' = -x \sin\theta + y \cos\theta \quad (4)$$

$$x' = x \cos\theta + y \sin\theta \quad (5)$$

Using the Gabor function, concept and filter design theory as a foundation direction, θ: depicts the Gabor function's direction of parallel stripes.

***Artificial Algae method (AAA)***

The AAA is a meta-heuristic optimizing method that draws inspiration from the characteristics and dynamic behavior of microalgae. An algal colony is a collection of algae that cohabit. Each colony is an example of a potential fix. Algae populations make up the number of people, which is represented as follows:

$$population = \begin{bmatrix} w_{1,1} & w_{1,2} & \dots & w_{1,C} \\ w_{2,1} & w_{2,2} & \vdots\vdots & w_{2,C} \\ \vdots & \vdots & \vdots & \vdots \\ w_{OM,1} & w_{OM,2} & \cdots & w_{OM}, C \end{bmatrix} \quad (6)$$

$$j^{th}\ algal\ colony\ (w_j) = [w_{j,1}, w_{j,2} \dots, w_{j,C}] \quad (7)$$

Where, $C$ denotes the dimensions of the algae communities, $PN$ is the count of algae communities in the overall population and $w_{ij}$ represents the algal cell in the $jth$ location of the algae population. A collection of algal cells that are thought to have solution dimensions make up an algal colony. The algae community travels in unison in the direction of a suitable habitat that provides nutrition. The algae population moves, changes and grows in an attempt to get into a better place. When the colony is positioned optimally, the best possible outcome is achieved. Throughout the identification process, the size of each algal colony is determined by the amount of light and nutrients that collects. All algae communities have a starting dimension of $(greatness\ H)$. The algae communities' development dynamics $\mu$ are equations 8 and 9.

$$\mu_j^S = \frac{\mu_{max}^S \times T^S}{L_t^S + T^S} \quad (8)$$

$$H_j^{s+1} = H_j^s + \mu_j^s H_j^s \quad (9)$$

Where $\mu_{max}^S$ at period t, maximum represents the highest specified growth rate and $L_t^S$ is the $H_j^S$ is the measurement of the $ith$ algae community at period $s$ and medium saturating characteristic at the period $s$. The three primary components of AAA are Adaption, helical movement and the evolutionary process.

- **Evolutionary process:**

When an algae community discovers an effective method it expands and increases. The algae populations will soon die if they are unable to develop and find an appropriate answer. Throughout the development of the algae, greatness $(H)$ is the criterion used for separating communities. The youngest algae population's randomized single dimension is destroyed and the corresponding component of the largest algae population is replicated in its place in equations 10 to 12.

$$biggest^s = \max\left(H_j^s\right)\ j = 1,2,..OM \tag{10}$$

$$smallest^s = \min\left(H_j^s\right)\ j = 1,2,...OM \tag{11}$$

$$smallest_n^s = biggest_n^s n = 1,2,..C \tag{12}$$

Where $biggest^s is$ the human population's largest algae community at period $s$, where $smallest^s$ is the population member that is youngest at period $s$.

- **Helical movement:**

Every process starts with a power calculation that takes the algae communities' beauty into account or normalizes it. Every algae colony's power determines how many times it travels helically in a given cycle. The colony's activity is closely correlated with the quantity of nutrients it gets from its surroundings. The algae population that discovers an improved approach experiences energy loss during the helical movement that is half $(e/2)$ of the beginning energy loss value. The algae population experiences losses of energy equal to the power loss factor $(e)$ if it is unable to come up with a better alternative.

$$\tau\left(w_j\right) = 2\pi\left(\sqrt[3]{\frac{3H_j}{4\pi}}\right)^2 \tag{13}$$

where the $ith$ algae colony's frictional area is represented by s $\tau\left(w_j\right)$. An algae colonies chosen by the competition technique has its three-dimensional $(p, r, and\ v)$ for the helical movement specified. Equations 14 to 16 are used to determine the movement's stepping length.

$$w_{ip}^{s+1} = w_{ip}^s + \left(w_{jp}^s - w_{ip}^s\right)\left(\Delta - \tau^t\left(W_j\right)\right)O \tag{14}$$

$$w_{ir}^{s+1} = w_{ir}^s + \left(w_{jr}^s w_{ir}^s\right)\left(\Delta - \tau^s\left(W_j\right)\right)\cos\alpha \tag{15}$$

$$w_{iv}^{s+1} = w_{iv}^s + \left(w_{ju}^s - w_{iu}^s\right)\left(\Delta - \tau^s\left(W_j\right)\right)\sin\theta \tag{16}$$

Where D is the shear stress, s $\tau^t(W_j)$ is the frictional area in the $ith$ algae community and x$w_{ip}^s, w_{ir}^s, and\ w_{iv}^s$ are the $x, y, and\ z$ positions of the $ith$ algae population at period $s$, $\alpha, \theta \in [0, 2\pi], o \in [-1, 1], \Delta$ Shear stress, loss of energy $e$ and adaption factor $Ap$ are the three variables in $AAA$. The adaption factor in the current study is 0.2, the loss of energy value is 0.3 and the shear stress value is 2.

- **Adaption:**

The stage in which a population that can function but not expand to a suitable size is considered to be the best colony is called adaption. In the beginning, every algae population has no dehydration. The algae colony's hunger level rises with each helical movement while it is unable to discover an improved option. Following every phase of the helical movement, the algae population exhibiting the greatest degree of hunger experiences a modification process in equations 17 to 18.

$$starving^s = maxB_j^s \quad (17)$$

$$starving^{s+1} = starving^s + (biggest^s - starving^s) \times rand \quad (18)$$

Where $starving^s$ represent the algae colonies with the maximum deprivation level at period $s$ and $B_j^s$ represent the level of starvation value of the algae population at period $s$. The application of the adaptability procedure at time $s$ is determined by the adaptability variable$(Ap)$. $Ap$ is a method-specific variable with a value of $0\ to\ 1$.

***Evolving Algorithms Motivated by Quantum Concepts***

The principles of quantum mechanics are the source of quantum computing. Quantum computing's superposition lowers the computational difficulty. One can leverage this capacity for processing in parallel to find solutions to issues. That requires examining big resolution areas. Nevertheless, these algorithms are unable to be implemented due to the lack of quantum machines. Thus, studies on integrating these methods with traditional techniques, including QEA, have been conducted and used to address optimization issues such as parameter estimation, filter design and the knapsack issue.

Despite having its foundation in the ideas and concepts of quantum computing, including quantum bits, permutation of states and quantum gates, QEA is an algorithm that evolves rather than a quantum algorithm. The simplest data unit in QEA is known as the Q-bit and it is defined as$[\alpha, \beta]^S$. The Q-bit related states' probabilities intensity are indicated by the complex values α

and β. The possibility that the Q-bit will be "0" is represented by α, while the possibility that it will be "1" is represented by$|\beta|^2$. The following defines each unique $w_j$ of QEA with m-bit:

$$w_j = \begin{bmatrix} \alpha_1 & \alpha_2 & \cdots & \alpha_m \\ \beta_1 & \beta_2 & \ldots & \beta_n \end{bmatrix} \tag{19}$$

Where $|\alpha_j|^2 + |\beta_j|^2 = 1,\ j = 1, 2, .. n$. For example, in a system Q consisting of three Q-bits and three distinct sets of intensities,

$$R = \begin{bmatrix} \frac{\sqrt{2}}{2} & \frac{\sqrt{2}}{2} & \frac{1}{2} \\ \frac{\sqrt{2}}{2} & -\frac{\sqrt{2}}{2} & \frac{\sqrt{3}}{2} \end{bmatrix} \tag{20}$$

Its circumstances are as follows:

$$\frac{1}{4}|000\rangle + \frac{\sqrt{3}}{4}|010\rangle - + \frac{\sqrt{3}}{4}|010\rangle + \frac{1}{4}|101\rangle + \frac{\sqrt{3}}{4}|101\rangle - \frac{1}{4}|110\rangle - \frac{\sqrt{3}}{4}|111\rangle$$

(21)

This indicates that the odds of residing in the various states are, in that order, $1/16, 3/16, 1/16, 3/16, 1/16, 1/16, and\ 3/16$. As a result, the three Q-bit systems mentioned above contain the data for eight states. To assess each person's performance in QEA for directing algorithm updates and addressing optimized difficulties, the appropriate expressed methods are required. By watching the Q-bits, a traditional binary answer can be formed.

In other words, a random number $\eta$ among [0, 1] is created for a bit $ri$ of the binaries individuals $r$ and it is contrasted against $\alpha_j$ of the Q-bit individuals p. Set $q_j = 0$ if $\alpha_j$ fulfills $|\alpha_j|^2 > \eta$ different, set $q_j = 1$.

$$\begin{cases} q_j = 0\ \ if\ |\alpha_j|^2 > \eta \\ q_j = 1\ \ if\ |\alpha_j|^2 \leq \eta \end{cases} \tag{22}$$

By examining the different states of the existing Q-bit responses, the complete binary solutions can be constructed after these stages.

Each person's fitness is assessed following the generation of the relevant traditional solutions. The Q-bit individuality is updated using a quantum rotation gate $Q(\theta_{id})$in the manner described below:

$$\begin{bmatrix} \alpha_{id} \\ \beta_{id} \end{bmatrix} = Q(\theta_{id}) \begin{bmatrix} \alpha_{id} \\ \beta_{id} \end{bmatrix} = \begin{bmatrix} \cos(\theta_{id}) & -\sin(\theta_{id}) \\ \sin(\theta_{id}) & \cos(\theta_{id}) \end{bmatrix} \cdot \begin{bmatrix} \alpha_{id} \\ \beta_{id} \end{bmatrix} \tag{23}$$

The direction of the rotation angle is denoted by $\theta_{id}$. Each Q-bit converges to the fitting states through the process of quantum rotation gate updating. The individual with the most effective

approach is chosen and if it turns out to be superior compared to the best solution that has been stored, the best solution will be modified. Rotational angle $\theta_{id}$ is an essential variable while the quantum rotation gate updates the individuals. It needs the theoretical foundation about the value of$\theta_{id}$, though. Typically, $\theta_{id}$ is described as:

$$\theta_{id} = t\,(\alpha_{id}, \beta_{id}) \cdot \Delta\theta_{id} \quad (24)$$

where $\Delta\theta_{id}$is the turning angle's amplitude and $t(\alpha_{id}, \beta_{id})$is the sign of $\theta_{id}$ which decides the orientation. The searching table in Table 1 determines the significance of $t(\alpha_{id}, \beta_{id})$ and $\Delta\theta_{id}$. The $d-th$ bit of the current solution's $i-th$ individual is represented by $ri_d$ in Table 1, while $b_d$ represents the $d-th$ bit of the best approach $b$.

**Table 1** The rotating angles calculation table for QEA

(Source: Author)

| $w\_id$ | $a\_c$ | $e(w\_j) > e(a)$ | $\Delta\theta\_id$ | $T(\alpha\_j, \beta\_j)$ | | | |
|---|---|---|---|---|---|---|---|
| | | | | $\alpha\_id\ \beta\_id > 0$ | $\alpha\_id\ \beta\_id < 0$ | $\alpha\_id = 0$ | $\beta\_id = 0$ |
| 0 | 0 | $False$ | 0 | 0 | 0 | 0 | 0 |
| 0 | 0 | $True$ | 0 | 0 | 0 | 0 | 0 |
| 0 | 1 | $False$ | 0 | 0 | $0-1$ | 0 | 0 |
| 0 | 1 | $True$ | $0.05\,\pi$ | $+1$ | $-1$ | 0 | $\pm1$ |
| 1 | 0 | $False$ | $0.01\,\pi$ | $+1$ | $+1$ | 0 | $\pm1$ |
| 1 | 0 | $True$ | $0.025\,\pi$ | 1 | $+1$ | $\pm1$ | 0 |
| 1 | 1 | $False$ | $0.005\,\pi$ | $-1$ | $+1$ | $\pm1$ | 0 |
| 1 | 1 | $True$ | $0.025\,\pi$ | $-1$ | 1 | $\pm1$ | 0 |

***Quantum artificial algae algorithm (QAAA)***

The Quantum Artificial Algae Algorithm (QAAA) improves MRI BT segmentation by imitating the behavior of algae and utilizing quantum computing principles. QAAA enhances accuracy and efficiency in the segmentation process by fusing the adaptability of artificial algae with the parallelism of quantum computing. This novel strategy has the potential to improve medical imaging and enable more accurate brain tumor identification and treatment planning. Algorithm 1 illustrates the Quantum artificial algae algorithm (QAAA).

**Algorithm 1: Quantum artificial algae algorithm (QAAA)**

```
procedure QAAA(initial_population, fitness_function, quantum_circuit):
Initialize quantum_register with qubits for representing solutions
Initialize classical_register for storing measurement results
for iteration in range(max_iterations):
for solution in initial_population:
quantum_circuit.initialize(solution, quantum_register)
apply_quantum_gates(quantum_circuit)
measure(quantum_register, classical_register)
fitness = fitness_function(classical_register)
update_fitness_score(solution, fitness)
selected_population = select_solutions(initial_population, fitness_scores)
crossover(selected_population, quantum_circuit)
mutate(selected_population, quantum_circuit)
initial_population = selected_population
return best_solution(initial_population)
```

## Results

### *Experimental setup*

The suggested approach has been implemented in this work using the Python platform. We need a portable computer with an Intel i6 microprocessor operating Windows 10, 100 GB hard drive and 32 GB of RAM.

### *Metrics and networks for evaluating effectiveness*

The measures of recall, specificity, accuracy, precision and F1-score are examined in this section. There is a comparison between the ResNet50, AlexNet and VGG16 models' classification performance. VGG16, AlexNet and ResNet50 models are used in the transfer learning methods on the Kaggle dataset (Amran et al. (2022)).

In MRI brain tumor segmentation, accuracy, precision, recall, F1-score and specificity are commonly used evaluation metrics to assess the performance of the segmentation algorithms. These metrics provide a quantitative measure of how well the algorithm is able to delineate as well as classify different regions of interest in medical images, such as tumor and non-tumor regions.

- **Accuracy:**

Accuracy is a statistic used to assess a segmentation algorithm's performance in the framework of MRI BT segmentation by calculating the overall correctness of the segmentation findings. The conventional categorization is the proportion of pixels correctly identified to the overall amount of pixels in the image.

$$Accuracy = \frac{Number\ of\ correctly\ classified\ pixels}{total\ number\ of\ pixels} \quad (25)$$

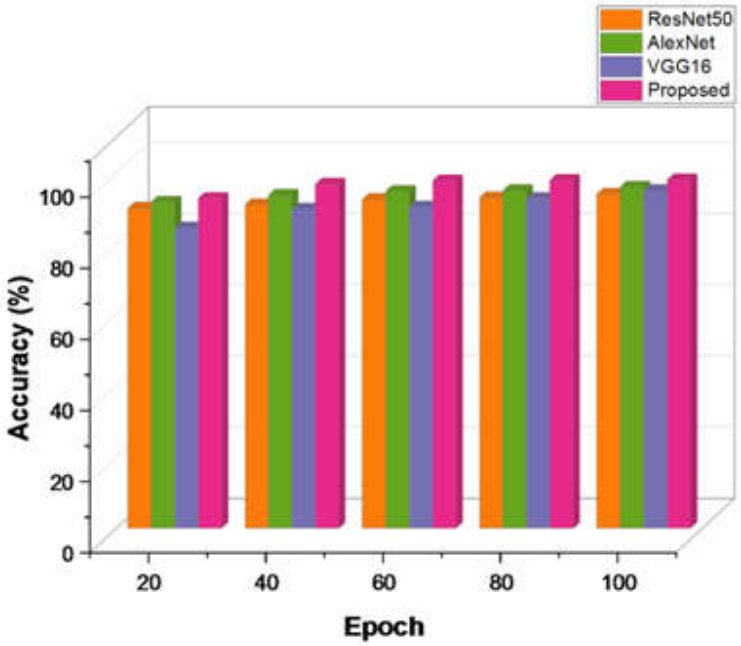


**Fig. 3** Results of accuracy

(Source: Author)

**Table 2** Values of accuracy

(Source: Author)

| Epoch | Accuracy (%) | | | |
|---|---|---|---|---|
| | **ResNet50** | **AlexNet** | **VGG16** | **Proposed** |
| 20 | 90 | 91.8 | 84.5 | 92.8 |
| 40 | 91 | 93.7 | 89.7 | 96.8 |
| 60 | 92.5 | 94.8 | 90.4 | 97.8 |
| 80 | 93 | 95 | 92.8 | 97.9 |
| 100 | 94 | 96 | 95 | 98 |

Equation 25 evaluates the accuracy with which a method suggests its position from the information at present. Table 2 and Fig 3 show the evaluation of the proposed and existing methods. In contrast to the existing approach ResNet (94%), AlexNet (96%) and VGG-16 (95%). If our suggested method achieves QAAA (98%), it is demonstrated that it is better than the existing approach for MRI BT segmentation.

- **Precision:**

Precision is a statistic used to evaluate the segmentation findings' correctness. It determines the proportion of actual positive forecasts to all positive cases that are anticipated.

$$Precision = \frac{True\ positive}{True\ positive + False\ positive} \quad (26)$$

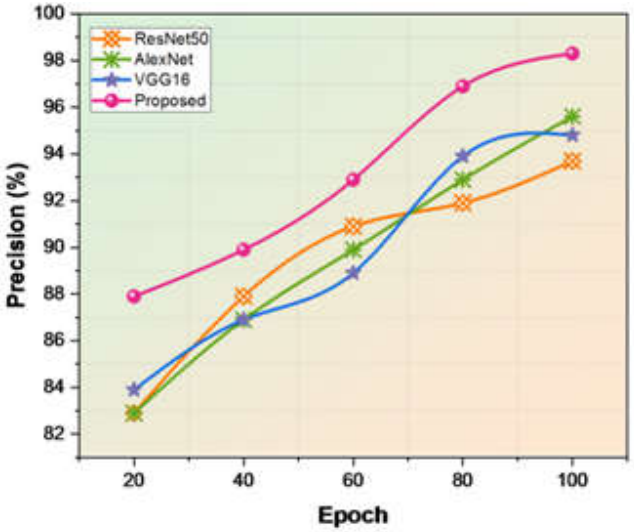


**Fig. 4** Results of precision

(Source: Author)

**Table 3** Values of precision

(Source: Author)

| Epoch | Precision (%) | | | |
|---|---|---|---|---|
| | ResNet50 | AlexNet | VGG16 | Proposed |
| 20 | 82.9 | 82.9 | 83.9 | 87.9 |
| 40 | 87.9 | 86.9 | 86.9 | 89.9 |
| 60 | 90.9 | 89.9 | 88.9 | 92.9 |
| 80 | 91.9 | 92.9 | 93.9 | 96.9 |
| 100 | 93.7 | 95.6 | 94.8 | 98.3 |

The calculation is performed utilizing the prescribed Equation 26. A comparison of the precision of the existing method and the proposed method is presented in Fig 4 and Table 3. In contrast to the popular methods scored ResNet (93.7%), AlexNet (95.6%) and VGG-16 (94.8%), respectively, the proposed strategy QAAA achieved (98.3%) precision. Therefore, the proposed technique performs better for BT segmentation from MRI.

- **Recall:**

A metric called recall is also called sensitivity or true positive rate is employed when categorizing brain cancers with magnetic resonance imaging (MRI) and other medical imaging techniques. Recall is important for medical diagnosis, particularly for brain tumor classification. It shows that all disease cases are detected by the algorithm and false negatives are reduced to the lowest.

$$Recall = \frac{True\ positive}{True\ positive + False\ negative} \quad (27)$$

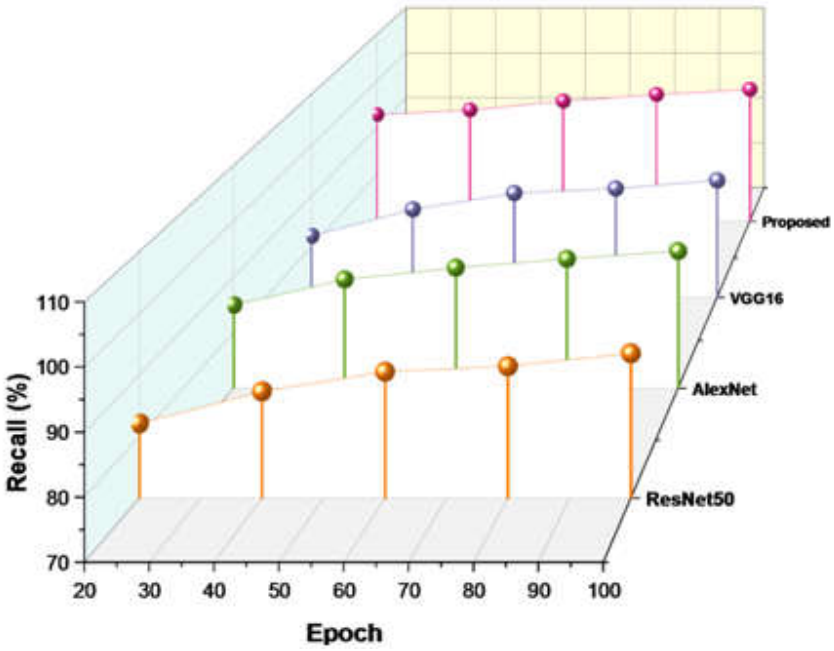


**Fig. 5** Results of recall

(Source: Author)

Fig 5 and Table 4 compare the recall equation 27 of the suggested method with the traditional approach. In contrast to the current approaches, ResNet, AlexNet and VGG-16 scored 93.5%, 94.6% and 93%; however, the suggested method, QAAA, scored 98.2%. This result directly contributes to the superior performance of the approach we have proposed.

**Table 4** Values of recall

(Source: Author)

| Epoch | Recall (%) | | | |
|---|---|---|---|---|
| | **ResNet50** | **AlexNet** | **VGG16** | **Proposed** |
| 20 | 82.1 | 84.9 | 82.1 | 92.8 |
| 40 | 87.3 | 89.5 | 87.3 | 93.8 |
| 60 | 90.5 | 91.6 | 90.5 | 95.7 |
| 80 | 91.4 | 93.2 | 91.4 | 97.1 |
| 100 | 93.5 | 94.6 | 93 | 98.2 |

- **Specificity:**

Specificity is a binary categorization metric that evaluates a model's capacity to accurately identify valid negatives among all real-world negative examples. subtract the entire amount of false positives and true negatives by the total number of true negatives to perform the computation. The specificity equation 28 is as follows:

$$Specificity = \frac{TN}{TN+FP} \quad (28)$$

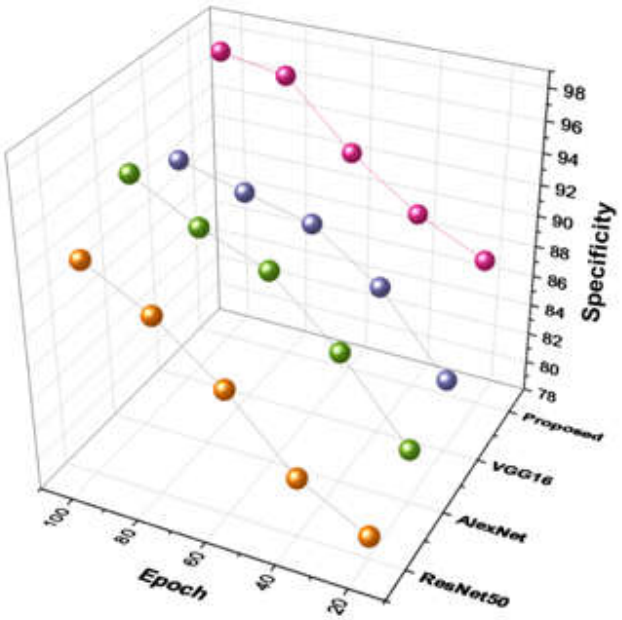


**Fig. 6** Results of specificity

(Source: Author)

**Table 5** Values of specificity

(Source: Author)

| Epoch | Specificity (%) | | | |
|---|---|---|---|---|
| | ResNet50 | AlexNet | VGG16 | Proposed |
| 20 | 79.5 | 81.6 | 82.9 | 87.9 |
| 40 | 81.9 | 86.7 | 87.9 | 89.9 |
| 60 | 86.3 | 90.7 | 90.9 | 92.9 |
| 80 | 89.7 | 92.3 | 91.9 | 96.9 |
| 100 | 92 | 94.6 | 93 | 97.6 |

Fig 6 and Table 5 compare the specificity of the suggested method with that of the traditional approach. Compared to the current approaches, ResNet, AlexNet and VGG-16 scored 92%, 94.6% and 93% on the different combinations, the proposed method, QAAA, scored 97.6%. It directly contributes to the method we have suggested performing more effectively.

- **F1-score:**

While MRI imaging is required to classify brain tumors, a statistic called the F1-score, or F1 measure, is employed to assess how well a binary classification model performs. It takes consideration for recall as well as precision. The following is the F1-score equation 29:

$$\text{F1-score} = 2\times\frac{Precision\times Recall}{Precision+Recall} \quad (29)$$

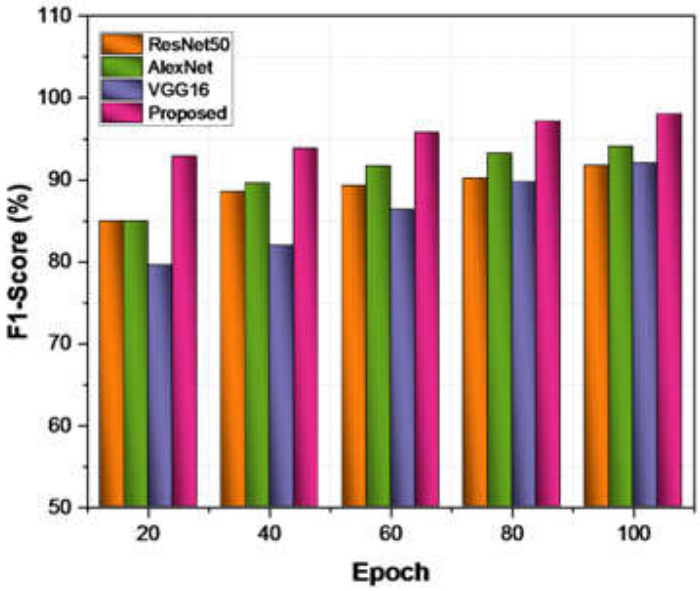


**Fig. 7** Results of F1-score (Source: Author)

**Table 6** Values of F1-score

(Source: Author)

| Epoch | F1-Score (%) | | | |
|---|---|---|---|---|
| | **ResNet50** | **AlexNet** | **VGG16** | **Proposed** |
| 20 | 84.9 | 84.9 | 79.5 | 92.8 |
| 40 | 88.5 | 89.5 | 81.9 | 93.8 |
| 60 | 89.2 | 91.6 | 86.3 | 95.7 |
| 80 | 90.1 | 93.2 | 89.7 | 97.1 |
| 100 | 91.7 | 94 | 92 | 98 |

In Fig 7 and Table 6, the suggested method is contrasted with the standard approach's F1-score. In contrast, the suggested method QAAA scored 98% whereas the well-known approaches ResNet, AlexNet and VGG-16 earned 91.7%, 94% and 92%, respectively. This outcome is related to the improved performance of our proposed technique.

**Conclusion**

In summary, the critical phase of MRI brain tumor segmentation in medical image processing was the object of our study. To accurately diagnose brain tumors, plan treatments and track tumor development, the suggested Quantum Artificial Algae Algorithm (QAAA) proved effective in recognizing and characterizing tumors in MRI data. We utilized a 253-image dataset (155 cancers and 98 non-tumor pictures) from Kaggle. To reduce intensity variations and ensure image comparability across various treatments, pixel value normalization was used as a preprocessing technique.Utilizing the Gabor filter technique, pertinent characteristics were extracted from the pre-processed data, demonstrating its usefulness as an assessment tool for brain tumor identification in MRI data. We proposed a model that addressed the trade-off between prospecting and exploiting by including a quantum-inspired computation technique. The initial rotation of a community of individuals to a location where optimal values could be more easily obtained was made easier by the application of a quantum rotation gate.We used Python 3.11 software to execute simulations and evaluate the efficiency of the proposed technique, yielding excellent performance figures. A remarkable 98.3% accuracy, 98.2% precision, 98.6% specificity, 97.6% recall and a 98% F1-score were attained by the QA method. These results demonstrate the applicability and importance of the QA model for MRI brain tumor segmentation. Challenges addressing different tumor forms and variations in imaging techniques require for more

investigation into reliable and flexible segmentation models. Artificial intelligence and machine learning algorithms can be included in MRI BT segmentation in the future to improve accuracy and speed which may enable individualized treatment plans and improve patient outcomes.

**Reference**


1. Ali, S., Li, J., Pei, Y., Khurram, R., Rehman, K.U. and Mahmood, T.: A comprehensive survey on brain tumor diagnosis using deep learning and emerging hybrid techniques with multi-modal MR image. Archives of computational methods in engineering, 29(7), pp.4871-4896, (2022). https://doi.org/10.1007/s11831-022-09758-z
2. Amian, M. and Soltaninejad, M.: Multi-resolution 3D CNN for MRI brain tumor segmentation and survival prediction. In Brainlesion: Glioma, Multiple Sclerosis, Stroke and Traumatic Brain Injuries: 5th International Workshop, BrainLes 2019, Held in Conjunction with MICCAI 2019, Shenzhen, China, October 17, 2019, Revised Selected Papers, Part I 5 (pp. 221-230), (2020) Springer International Publishing. https://doi.org/10.1007/978-3-030-46640-4_21
3. Amran, G.A., Alsharam, M.S., Blajam, A.O.A., Hasan, A.A., Alfaifi, M.Y., Amran, M.H., Gumaei, A. and Eldin, S.M.: Brain Tumor Classification and Detection Using Hybrid Deep Tumor Network. Electronics, 11(21), p.3457, (2022). https://doi.org/10.3390/electronics11213457
4. Amran, G.A., Alsharam, M.S., Blajam, A.O.A., Hasan, A.A., Alfaifi, M.Y., Amran, M.H., Gumaei, A. and Eldin, S.M.: Brain Tumor Classification and Detection Using Hybrid Deep Tumor Network. Electronics, 11(21), p.3457, (2022). https://doi.org/10.3390/electronics11213457
5. Ballestar, L.M. and Vilaplana, V.: October. MRI brain tumor segmentation and uncertainty estimation using 3D-UNet architectures. In International MICCAI Brainlesion Workshop (pp. 376-390), (2020). Cham: Springer International Publishing. https://doi.org/10.1007/978-3-030-72084-1_34
6. Biratu, E.S., Schwenker, F., Ayano, Y.M. and Debelee, T.G.: A survey of brain tumor segmentation and classification algorithms. Journal of Imaging, 7(9), p.179, (2021). https://doi.org/10.3390/jimaging7090179
7. Brahim, I., Fourer, D., Vigneron, V. and Maaref, H.: November. Deep learning methods for MRI brain tumor segmentation: a comparative study. In 2019 Ninth International

Conference on Image Processing Theory, Tools and Applications (IPTA) (pp. 1-6), (2019). IEEE. https://doi.org/10.1109/IPTA.2019.8936077

8. Chahal, P.K., Pandey, S. and Goel, S.: A survey on brain tumor detection techniques for MR images. Multimedia Tools and Applications, 79, pp.21771-21814, (2020). https://doi.org/10.3390/jimaging7090179
9. Chen, B., Zhang, L., Chen, H., Liang, K. and Chen, X.: A novel extended Kalman filter with support vector machine-based method for the automatic diagnosis and segmentation of brain tumors. Computer Methods and Programs in Biomedicine, 200, p.105797, (2021). https://doi.org/10.1016/j.cmpb.2020.105797
10. Chen, H., Qin, Z., Ding, Y., Tian, L. and Qin, Z.: Brain tumor segmentation with a deep convolutional symmetric neural network. Neurocomputing, 392, pp.305-313, (2020). https://doi.org/10.1016/j.neucom.2019.01.111
11. Colman, J., Zhang, L., Duan, W. and Ye, X.: DR-Unet104 for Multimodal MRI brain tumor segmentation. In Brainlesion: Glioma, Multiple Sclerosis, Stroke and Traumatic Brain Injuries: 6th International Workshop, BrainLes 2020, Held in Conjunction with MICCAI 2020, Lima, Peru, October 4, 2020, Revised Selected Papers, Part II 6 (pp. 410-419), (2021). Springer International Publishing. https://doi.org/10.1007/978-3-030-72087-2_36
12. Giacomello, E., Loiacono, D. and Mainardi, L.: July. Brain MRI tumor segmentation with adversarial networks. In 2020 International Joint Conference on Neural Networks (IJCNN) (pp. 1-8), (2020). IEEE. https://doi.org/10.1109/IJCNN48605.2020.9207220
13. Haq, A.U., Li, J.P., Khan, S., Alshara, M.A., Alotaibi, R.M. and Mawuli, C.: DACBT: Deep learning approach for classification of brain tumors using MRI data in IoT healthcare environment. Scientific Reports, 12(1), p.15331, (2022). https://doi.org/10.1038/s41598-022-19465-1
14. Kao, P.Y., Shailja, S., Jiang, J., Zhang, A., Khan, A., Chen, J.W. and Manjunath, B.S.: Improving patch-based convolutional neural networks for MRI brain tumor segmentation by leveraging location information. Frontiers in neuroscience, 13, p.1449, (2020) https://doi.org/10.3389/fnins.2019.01449

15. Khalil, H.A., Darwish, S., Ibrahim, Y.M. and Hassan, O.F.:3D-MRI brain tumor detection model using modified version of level set segmentation based on dragonfly algorithm. Symmetry, 12(8), p.1256, (2020). https://doi.org/10.3390/sym12081256
16. Kollam, S., Prasad, C.R., Ajayan, J., Malathy, V. and Subbarao, A.: Brain tumor MRI image segmentation using an optimized multi-kernel FCM method with a pre-processing stage. Multimedia Tools and Applications, 82(14), pp.20741-20770, (2023). https://doi.org/10.1007/s11042-022-14045-x
17. Kuraparthi, S., Reddy, M.K., Sujatha, C.N., Valiveti, H., Duggineni, C., Kollati, M. and Kora, P.: Brain Tumor Classification of MRI Images Using Deep Convolutional Neural Network. Traitement du Signal, 38(4), (2021). https://doi.org/10.18280/ts.380428
18. Kurmi, Y. and Chaurasia, V.: Classification of magnetic resonance images for brain tumor detection. IET Image Processing, 14(12), pp.2808-2818, (2020). https://doi.org/10.1049/iet-ipr.2019.1631
19. Magadza, T. and Viriri, S.: Deep learning for brain tumor segmentation: a survey of the state-of-the-art. Journal of Imaging, 7(2), p.19, (2021). https://doi.org/10.3390/jimaging7020019
20. Myronenko, A.: 3D MRI brain tumor segmentation using autoencoder regularization. In Brainlesion: Glioma, Multiple Sclerosis, Stroke and Traumatic Brain Injuries: 4th International Workshop, BrainLes 2018, Held in Conjunction with MICCAI 2018, Granada, Spain, September 16, 2018, Revised Selected Papers, Part II 4 (pp. 311-320), (2019). Springer International Publishing. https://doi.org/10.1007/978-3-030-11726-9_28
21. Ottom, M.A., Rahman, H.A. and Dinov, I.D.: Znet: deep learning approach for 2D MRI brain tumor segmentation. IEEE Journal of Translational Engineering in Health and Medicine, 10, pp.1-8, (2022). https://doi.org/10.1109/JTEHM.2022.3176737
22. Petralia, F., Tignor, N., Reva, B., Koptyra, M., Chowdhury, S., Rykunov, D., Krek, A., Ma, W., Zhu, Y., Ji, J., and Calinawan, A.: Integrated proteogenomic characterization across major histological types of pediatric brain cancer. Cell, 183(7), pp.1962-1985, (2020). https://doi.org/10.1016/j.cell.2020.10.044
23. Senan, E.M., Jadhav, M.E., Rassem, T.H., Aljaloud, A.S., Mohammed, B.A. and Al-Mekhlafi, Z.G.: Early diagnosis of brain tumor MRI images using hybrid techniques

between deep and machine learning. Computational and Mathematical Methods in Medicine, (2022). https://doi.org/10.1155/2022/8330833

24. Sheng, N., Liu, D., Zhang, J., Che, C. and Zhang, J.: Second-order ResU-Net for automatic MRI brain tumor segmentation. Mathematical biosciences and engineering, 18(5), pp.4943-4960 ( 2021). http://dx.doi.org/10.3934/mbe.2021251
25. Srinivasa Reddy, A. and Chenna Reddy, P.: MRI brain tumor segmentation and prediction using modified region growing and adaptive SVM. Soft Computing, 25, pp.4135-4148, (2021). https://doi.org/10.1007/s00500-020-05493-4
26. Tataei Sarshar, N., Ranjbarzadeh, R., Jafarzadeh Ghoushchi, S., de Oliveira, G.G., Anari, S., Parhizkar, M. and Bendechache, M.: October. Glioma Brain Tumor Segmentation in Four MRI Modalities Using a Convolutional Neural Network and Based on a Transfer Learning Method. In Brazilian Technology Symposium (pp. 386-402), (2021). Cham: Springer International Publishing. https://doi.org/10.1007/978-3-031-04435-9_39
27. Thaha, M.M., Kumar, K.P.M., Murugan, B.S., Dhanasekeran, S., Vijayakarthick, P. and Selvi, A.S.: Brain tumor segmentation using convolutional neural networks in MRI images. Journal of Medical Systems, 43, pp.1-10, (2019). https://doi.org/10.1007/s10916-019-1416-0
28. Wu, J., Zhou, L., Gou, F. and Tan, Y.: A residual fusion network for osteosarcoma MRI image segmentation in developing countries. Computational Intelligence and Neuroscience, (2022). https://doi.org/10.1155/2022/7285600
29. Yamanakkanavar, N., Choi, J.Y. and Lee, B.: MRI segmentation and classification of the human brain using deep learning for diagnosis of Alzheimer's disease: a survey. Sensors, 20(11), p.3243, (2020). https://doi.org/10.3390/s20113243
30. Zhang, J., Jiang, Z., Dong, J., Hou, Y. and Liu, B.: Attention gate resU-Net for automatic MRI brain tumor segmentation. IEEE Access, 8, pp.58533-58545, (2020). https://doi.org/10.1109/ACCESS.2020.2983075